The Ground-Truth Problem for Satellite Estimates of Rain Rate

GERALD R. NORTH, JUAN B. VALDÉS,* EUNHO HA,† AND SAMUEL S. P. SHEN**

Climate System Research Program, Texas A&M University, College Station, Texas

9 March 1993 and 7 January 1994

ABSTRACT

In this paper a scheme is proposed to use a point raingage to compare contemporaneous measurements of rain rate from a single-field-of-view estimate based on a satellite remote sensor such as a microwave radiometer. Even in the ideal case the measurements are different because one is at a point and the other is an area average over the field of view. Also the point gauge will be located randomly inside the field of view on different overpasses. A space–time spectral formalism is combined with a simple stochastic rain field to find the mean-square deviations between the two systems. It is found that by combining about 60 visits of the satellite to the ground-truth site, the expected error can be reduced to about 10% of the standard deviation of the fluctuations of the systems alone. This seems to be a useful level of tolerance in terms of isolating and evaluating typical biases that might be contaminating retrieval algorithms.

1. Introduction

With a number of satellites presently orbiting with microwave radiometers (e.g., Wilheit et al. 1991) on board and several set for launch in the next decade (e.g., Simpson et al. 1988), the stage is set for an era of rain data collection from these observing systems. A nagging problem in the satellite estimation of rain rate is the issue of ground truth. How can a ground-based measurement be compared with its satellite estimate with sufficient accuracy that algorithms can be checked? This paper considers a strategy that can be used to check the calibration of a retrieval algorithm as it applies to a single field of view (FOV, also referred to as a footprint) repeatedly visiting a site where a point gauge is located. For an individual measurement we might expect the satellite estimate to be rather poor since there is known to be a large amount of variability of rain rate within even a typical FOV (typically about 20 km across). But if such a measurement comparison is made many times, say over the course of a month or two, the average error variance is expected to be reduced inversely by the number of visits. This method is convenient since in principle we can easily continue to add to our database, thus sharpening our histogram of the differences between the satellite estimate and the gauge measurement. How many such visits are needed to ensure that the difference between the satellite measurements and the point gauge measurements will be small enough to assess the magnitude of biases in the algorithm to within a given tolerance?

The microwave radiometer estimates the rain rate by measuring the upwelling radiation from an atmospheric column. In the ideal case this represents a column average of the rain rate over the projection of the FOV onto the ground for the sensor. Such a measurement is not to be compared with the instantaneous rain rate at the surface but rather some kind of time average at the surface, since it takes raindrops several minutes to fall from the top of the column to the surface. This is very fortunate since instantaneous rain rates are notoriously variable in space and the effect of time averaging is to smooth considerably the spatial variability of the field. Hence, the comparison in our scheme is between the satellite estimate for an FOV and a few-minute time-averaged measurement from a raingage. The number of minutes used in the time average is open to question, but for averages ranging from 1 to 10 min there should be no appreciable bias introduced in measuring a mean rain rate over many cases. Here we are thinking of the point gauge as an estimator of the FOV area (and column) average. We study the dispersion of the distribution of differences for a range of time averages including the special case of zero duration averages. In our derivation we consider the zero duration or instantaneous comparison case in parallel to the time-averaged case for pedagogical reasons, since this singular limit is useful in understanding the sensitivity to small-scale effects.

* Current affiliation: Department of Civil Engineering, Texas A&M University, College Station, Texas.

† Current affiliation: Department of Statistics, Enje University, Pusan, Republic of Korea.

** Current affiliation: Department of Mathematics, University of Alberta, Edmonton, Alberta, Canada.

Corresponding author address: Dr. Gerald R. North, Texas A&M University, Climate System Research Program, Texas A&M University, College Station, TX 77843-3150.

In this paper we consider a few numerical examples that are likely to be useful in actual ground-truth programs. For example, the computations are presented for a variety of FOV shapes, such as circular disk, rectangle, and ellipse. The approach involving point gauges is only to be one aspect of a larger program that will employ radars and other means of estimating area averages near the ground. The advantage of the point gauge project proposed here is that it does not introduce the inevitably controversial algorithms associated with estimating the rain rate from a "ground truth" measurement such as that derived from radar. We think that radar will be the ultimate "bearer" of ground truth, but we think it essential to consider some alternatives to ward off criticism that will be directed at the radar measurements. We hasten to add that our comparison method can be applied to a very broad class of problems even beyond the case of precipitation fields. For example, the radar–point gauge problem can be considered with our formalism, and we intend to do so in future studies.

In this present study we will introduce a mean-square error formalism that has proven useful in the satellite sampling error problem (North and Nakamoto 1989; hereafter referred to as NN) and provide estimates of the number of visits necessary to make a useful bias assessment. Our calculations are still tentative, since we base them on some rather simple models of rain fields that are tuned to the GATE [GARP (Global Atmospheric Research Program) Atlantic Tropical Experiment] dataset (see NN for references). We look forward to improved estimates of rain field properties (space–time spectra) that can be fed into our scheme to improve its applicability to particular climatological regions or observation designs.

Consider a random field $\psi(\mathbf{r}, t)$ defined in the $\mathbf{r} = (x, y)$ plane and along the time axis t. Let the ensemble average of $\psi(\mathbf{r}, t)$ be zero and its variance at a point in space be σ^2. The random variable $\psi(\mathbf{r}, t)$ is assumed to be weakly statistically homogeneous in space and time; that is, the lagged covariance is a function only of $\xi = |\mathbf{r} - \mathbf{r}|$ and $\tau = |t - t'|$. We denote the lagged covariance by

$$\langle \psi(\mathbf{r}, t)\psi(\mathbf{r}', t)\rangle = \sigma^2\rho(\xi, \tau), \tag{1}$$

where $\rho(\xi, \tau)$ is the space–time lagged autocorrelation with $\rho(0, 0) = 1$. The normalized spectral density function for the random field $\psi(\mathbf{r}, t)$ is defined as the Fourier transform of the autocorrelation function $\rho(\xi, \tau)$:

$$S(\nu, f) = \iiint \rho(\xi, \tau) \exp[2\pi i(\xi\cdot\nu + f\tau)]d^2\xi d\tau. \tag{2}$$

The inverse Fourier transform of $S(\nu, f)$ is

$$\rho(\xi, \tau) = \iiint S(\nu, f) \times \exp[-2\pi i(\xi\cdot\nu + f\tau)]d^2\nu df. \tag{3}$$

As a typical experiment we envision a point gauge located at some fixed site $\mathbf{r}_g$. The satellite passes over the site, and one of the FOVs in the swath along the ground track covers the gauge. We have two measurements taken from the nth visit, Ψ_s^n and Ψ_g^n, where the subscripts denote satellite and gauge, respectively. We form the difference between the two measurements and call this the error $e_n = \Psi_s^n - \Psi_g^n$ for the nth visit. Next we form the ensemble mean of the squared error

$$\epsilon_1^2 = \langle e_n^2\rangle. \tag{4}$$

The ensemble is to include all the possible realizations of the rain-rate field along with all the uniformly distributed locations of the centroid of the FOV. If the rain-rate field is such that each visit of the FOV to the gauge is statistically independent (autocorrelation times for a typical area the size of an FOV are only an hour or so whereas revisit intervals for a satellite are an order of magnitude longer), then the average mean-square error for N visits is

$$\epsilon_N^2 = \frac{\epsilon_1^2}{N}. \tag{5}$$

The main purpose of this paper is to find the value of N such that ϵ_N^2 is less than some preassigned tolerance.

2. Mean-square error for a single visit

In this section we set up the error variances for both the instantaneous and time-averaged cases in parallel to bring out their similarities and differences.

a. Introduction

The error variance is derived for an FOV having region R, the domain of a satellite footprint on the surface of the earth. The FOV average of $\psi(\mathbf{r}, t)$ over the FOV of nth visit is

$$\Psi_s = \frac{1}{A}\int_R \psi(\mathbf{r}, t)d^2\mathbf{r}, \tag{6}$$

where R is the FOV of this visit and A is the area of R. The variance of FOV averages σ_A^2 can be expressed in terms of the point variance and the normalized spectral density,

$$\sigma_A^2 = \frac{1}{A^2}\left\langle\left[\int_R \psi(\mathbf{r}, t)d^2\mathbf{r}\right]\left[\int_R \psi(\mathbf{r}', t)d^2\mathbf{r}'\right]\right\rangle. \tag{7}$$

Substituting the definition of the correlation function, we have

$$\sigma_A^2 = \frac{\sigma^2}{A^2}\int_R\int_R \rho(\xi, 0)d^2\mathbf{r}\,d^2\mathbf{r}'. \tag{8}$$

Using the inverse Fourier transform of the spectral density function and changing the order of the integration yields

$$\sigma_A^2 = \sigma^2 \int_{-\infty}^{\infty} \int_{-\infty}^{\infty} S(\nu) |D_R(\nu)|^2 d^2\nu, \quad (9)$$

where

$$S(\nu) = \int_{-\infty}^{\infty} S(\nu, f) df \quad (10)$$

is the contemporaneous spatial spectral density of the rain field defined by (2), and

$$D_R(\nu) = \frac{1}{A} \int_R \exp(2\pi i \nu \cdot \mathbf{r}) d^2\mathbf{r}. \quad (11)$$

In our study three ideal FOV shapes—the rectangular, circular, and elliptical footprints—are studied. The function $D_R(\nu)$ is defined for three FOV shapes as

$$D_R(\nu) = G(\nu_x a) G(\nu_y b)$$

rectangle: $R = [-a/2, a/2] \times [-b/2, b/2]$, (12)

$$D_R(\nu) = \frac{1}{\pi \nu a} J_1(2\pi a \nu)$$

circular disc: $R = \{(x, y) | r = (x^2 + y^2)^{1/2} \leq a\}$, (13)

$$D_R(\nu) = \frac{1}{\pi[(a\nu_x)^2 + (b\nu_y)^2]^{1/2}} \times J_1\{2\pi[(a\nu_x)^2 + (b\nu_y)^2]\}^{1/2}$$

ellipse: $R = \left\{(x, y) \left| \frac{x^2}{a^2} + \frac{y^2}{b^2} \leq 1 \right.\right\}$, (14)

where $G(x) \equiv (\pi x)^{-1} \sin(\pi x)$, $\nu = (\nu_x^2 + \nu_y^2)^{1/2}$, and $J_1(z)$ is the first-order Bessel function. Fourier integrals over the FOV are familiar from physical optics as diffraction patterns for the corresponding apperture shapes. Derivations of these functions are sketched in the appendix.

b. Averaging over centroid location of FOV

As outlined in the introduction, the first step is to evaluate the error variance for one gauge inside a satellite footprint. The centroid of the FOV on each visit is located randomly with respect to the position of the gauge. Equivalently, we take the centroid to be fixed and consider the gauge location to be a random variable uniformly distributed over the FOV:

$$P(\mathbf{r}_g) = \begin{cases} \frac{1}{A}, & \text{when } \mathbf{r}_g \in R \\ 0, & \text{otherwise.} \end{cases}$$

We seek the expectation value of the error variance with respect to all possible centroid locations uniformly distributed inside R. To compute the expectation value of the error variance, one will need to deal with the following factors:

$$E[\cos(2\pi \nu \cdot \mathbf{r}_g)] = D_R(\nu), \quad (15)$$

$$E[\sin(2\pi \nu \cdot \mathbf{r}_g)] = 0. \quad (16)$$

c. Mean-square error: No time averaging

For the problem posed here there is one gauge located at $\mathbf{r}_g$ and the satellite estimate based on R, which is the FOV for a visit

$$\Psi_s = \frac{1}{A} \int_R \psi(\mathbf{r}, t) d^2\mathbf{r}. \quad (17)$$

The instantaneous precipitation rate from this gauge measurement is

$$\Psi_g = \psi(\mathbf{r}_g, t) = \frac{1}{A} \int_R \psi(\mathbf{r}, t) K(\mathbf{r}) d^2\mathbf{r}, \quad (18)$$

where $K(\mathbf{r}) = A\delta(\mathbf{r} - \mathbf{r}_g)$. For an individual visit the error variance is

$$\epsilon_1^2 = \langle (\Psi_s - \Psi_g)^2 \rangle. \quad (19)$$

In practice, we seek to reduce this error variance by resampling N independent times. In a similar manner to the procedure followed for σ_A^2, we can show

$$\epsilon_1^2 = \sigma^2 \int_{-\infty}^{\infty} \int_{-\infty}^{\infty} S(\nu) |D_\epsilon(\nu)|^2 d^2\nu, \quad (20)$$

where

$$D_\epsilon(\nu) = D_R(\nu) - \exp(2\pi i \nu \cdot \mathbf{r}_g). \quad (21)$$

Parenthetically, it can be shown that the error variance is a minimum when the centroid of the FOV is placed at the location of the gauge; that is, $\mathbf{r}_g = 0$.

Since the gauge location is distributed uniformly within the FOV, we seek the expectation value of ϵ_1^2 with respect to all possible locations of the gauge. To compute the expected value of ϵ_1^2, one only needs to deal with the factor $|D_\epsilon(\nu)|^2$. From (2), (15), and (16), we have

$$E[|D_\epsilon(\nu)|^2] = 1 + D_R^2(\nu) - 2D_R(\nu) E[\cos(2\pi \nu \cdot \mathbf{r}_g)] = 1 - D_R^2(\nu). \quad (22)$$

Therefore,

$$E_1^2 = E(\epsilon_1^2) = \sigma^2 \iint S(\nu)[1 - D_R^2(\nu)] d^2\nu. \quad (23)$$

Ultimately we want to know the ratio of the error variance to the variance of an FOV average

$$V_1^2 = \frac{E_1^2}{\sigma_A^2}, \quad (24)$$

where E_1^2 and σ_A^2 are given by expressions (23) and (9), respectively. We refer to V_1^2 as the dimensionless error variance for the contemporaneous measurement. We chose σ_A^2 as a normalization because it is a convenient quantity that can be measured independently.

It is also natural that we would want our histogram of differences to be narrow compared to this histogram describing the local climatological variance. Thus,

$$V_1^2 = \frac{E_1^2}{\sigma_A^2} = \frac{\iint S(\nu)d^2\nu}{\iint S(\nu)D_R^2(\nu)d^2\nu} - 1. \quad (25)$$

Since

$$|D_R(\nu)|^2 \leq 1, \quad (26)$$

it is guaranteed that the right-hand side of (25) is nonnegative. When the spectrum is normalized according to

$$\iint S(\nu)d^2\nu = \rho(0, 0) = 1, \quad (27)$$

the dimensionless error variance can be written as

$$V_1^2 = \frac{1}{\iint S(\nu)D_R^2(\nu)d^2\nu} - 1. \quad (28)$$

d. Mean-square error: Time-average case

In practice, the satellite measures the column average of rain rate, which is equivalent to a time average of a few minutes at the surface. In this case we form the "truth" by taking a short time average of the gauge measurement over an interval T for a visit, which might typically be a few minutes,

$$\Psi_{gT} = \frac{1}{T}\int_0^T \psi(\mathbf{r}_g, t)dt \quad (29)$$

or

$$\Psi_{gT} = \frac{1}{AT}\int_0^T \int_R K(\mathbf{r})\psi(\mathbf{r}, t)d^2\mathbf{r}\,dt, \quad (30)$$

where $K(\mathbf{r}, t) = A\delta(\mathbf{r} - \mathbf{r}_g)$ is a kernel representative of the design. The satellite estimate of the T-long average for a visit consists of

$$\Psi_{sT} = \frac{1}{AT}\int_0^T \int_R \psi(\mathbf{r}, t)d^2\mathbf{r}\,dt. \quad (31)$$

For the two measurements, Ψ_{gT} and Ψ_{sT}, the subscripts emphasize the time average of the gauge and satellite measurement, respectively. We form the error variance

$$\epsilon_{1T}^2 = \langle(\Psi_{sT} - \Psi_{gT})^2\rangle, \quad (32)$$

which can be written

$$\epsilon_{1T}^2 = \frac{1}{A^2T^2}\int\int\int\int\int\int \langle\psi(\mathbf{r}, t)\psi(\mathbf{r}', t')\rangle \times [1 - K(\mathbf{r})][1 - K(\mathbf{r}')]d^2\mathbf{r}\,dt d^2\mathbf{r}'dt'. \quad (33)$$

Using the Fourier representation, we may write

$$\epsilon_{1T}^2 = \sigma^2 \iiint S(\nu, f)|D_{\epsilon T}(\nu, f)|^2 d^2\nu df, \quad (34)$$

where

$$D_{\epsilon T}(\nu, f) = G(fT)[D_R(\nu) - \exp(2\pi i\nu\cdot\mathbf{r}_g)] = G(fT)D_\epsilon(\nu), \quad (35)$$

and the function G is defined in section 2a; that is,

$$G(x) = \frac{\sin(\pi x)}{\pi x}. \quad (36)$$

We can write

$$\epsilon_{1T}^2 = \sigma^2 \iint S_T(\nu)|D_\epsilon(\nu)|^2 d^2\nu, \quad (37)$$

where $D_\epsilon(\nu)$ is the design filter for the instantaneous comparisons defined in section 2c and

$$S_T(\nu) = \int G^2(\pi fT)S(\nu, f)df. \quad (38)$$

Note that the mean-square error for the instantaneous comparisons ($T \to 0$) is

$$\epsilon_1^2 = \sigma^2 \iint S(\nu)|D_\epsilon(\nu)|^2 d^2\nu. \quad (39)$$

It is clear that the effect of time averaging is to low pass the spatial information, removing much of the small-scale variability. Not surprisingly, it can be shown that the mean-square error ϵ_{1T}^2 is a minimum at the center of the FOV; that is, $\mathbf{r}_g = 0$. With the expected value of $|D_\epsilon|^2$ in (22), we can compute the expected value of ϵ_{1T}^2 with respect to all possible locations of the gauge

$$E_{1T}^2 = \sigma^2 \iint S_T(\nu)[1 - D_R^2(\nu)]d^2\nu. \quad (40)$$

A useful dimensionless measure of the error variance that can be used to see the effect of FOV size is the ratio of the expected error variance to the variance of the time-averaged gauge measurement

$$W_{1T}^2 = \frac{E_{1T}^2}{\sigma_{gT}^2}, \quad (41)$$

where

$$\sigma_{gT}^2 = \langle\Psi_{gT}^2\rangle = \sigma^2 \iiint S(\nu, f)G^2(\pi fT)d^2\nu df = \sigma^2 \iint S_T(\nu)d^2\nu. \quad (42)$$

The measure W_{1T}^2 can be written from (40) and (42),

$$W_{1T}^2 = 1 - \frac{\iint S_T(\nu)D_R^2(\nu)d^2\nu}{\iint S_T(\nu)d^2\nu}. \quad (43)$$

Another measure of evaluating the error variance is the ratio of expected error variance to the variance of the satellite estimate

$$V_{1T}^2 = \frac{E_{1T}^2}{\sigma_A^2}, \tag{44}$$

where σ_A^2 is given by (9). Therefore, we have from (9) and (40),

$$V_{1T}^2 = \frac{\iint S_T(\nu)[1 - D_R^2(\nu)]d^2\nu}{\iint S(\nu)D_R^2(\nu)d^2\nu}. \tag{45}$$

A measure V_{1T}^2 is a useful dimensionless variance of expected satellite estimation error.

3. Numerical examples

In this section, we evaluate the error variance with the noise-forced diffusive rain model for the two designs: comparing snapshots and comparing column averages. Consider the model rain field $\psi(\mathbf{r}, t)$ generated by the process governed by

$$\tau_0 \frac{\partial \psi}{\partial t} - \lambda_0^2 \nabla^2 \psi + \psi = F(\mathbf{r}, t), \tag{46}$$

where τ_0 is a timescale and λ_0 is a length scale, both inherent to the field; F is a noise forcing function that might, for example, be white (or very broadband) in both space and time. The space–time spectrum of the noise-forced diffusive rain model is

$$S(\nu, f) = \frac{\alpha}{4\pi^2\tau_0^2 f^2 + (1 + 4\pi^2\lambda_0^2\nu^2)^2}, \tag{47}$$

where $\nu = |\boldsymbol{\nu}|$ and

$$\alpha = \frac{8\pi\tau_0\lambda_0^2}{\ln(1 + 4\pi^2\lambda_0^2\nu_c^2)^2}$$

is a normalization factor such that $\rho(0, 0) = 1$. For the GATE data of precipitation, these τ_0 and λ_0 take values around 12 h and 40 km, respectively (see NN). The cutoff $\nu_c = |\boldsymbol{\nu}_c|$ is to be thought of here as the smallest scale in the white noise forcing of the field. Taking this parameter small but finite keeps the point variance σ^2 from blowing up. An important property of any scheme is that it be insensitive to the cutoff parameter.

a. *No time averaging*

For the noise-forced diffusive rain model, we have

$$S(\nu) = \int_{-\infty}^{\infty} S(\nu, f)df = \frac{\alpha}{2\tau_0(1 + 4\pi^2\lambda_0^2\nu^2)}. \tag{48}$$

The dimensionless error variance is

$$V_1^2 = \frac{E_1^2}{\sigma_A^2} = \frac{\iint S(\nu)d^2\nu}{\iint S(\nu)D_R^2(\nu)d^2\nu} - 1$$

$$= \frac{\int_0^{2\pi}\int_0^{\nu_c} \nu/(1 + 4\pi^2\lambda_0^2\nu^2)d\nu d\theta}{\int_0^{2\pi}\int_0^{\nu_c} \nu D_R^2(\nu)/(1 + 4\pi^2\lambda_0^2\nu^2)d\nu d\theta} - 1. \tag{49}$$

Not surprisingly, the dimensionless error variance diverges as the wavenumber cutoff value ν_c goes to ∞. This comes about because the instantaneous point variance in the damped diffusion model with no cutoff diverges. While a more realistic rain field model might not have this property, it points out the sensitivity to the high wavenumber behavior of the field.

b. *Time-averaging case*

Results for the two measures of dimensionless error variance for one visit in section 2d are given by

$$W_{1T}^2 = 1 - \frac{\iint S_T(\nu)D_R^2(\nu)d^2\nu}{\iint S_T(\nu)d^2\nu}, \tag{50}$$

$$V_{1T}^2 = \frac{\iint S_T(\nu)[1 - D_R^2(\nu)]d^2\nu}{\iint S(\nu)D_R^2(\nu)d^2\nu}. \tag{51}$$

Here $S_T(\nu)$ is given by

$$S_T(\nu) = \int_{-\infty}^{\infty} \frac{\sin^2(\pi f T)}{(\pi f T)^2} \times \frac{\alpha}{4\pi^2\tau_0^2 f^2 + (1 + 4\pi^2\lambda_0^2\nu^2)^2} df. \tag{52}$$

Using the complex contour integral, we can derive

$$S_T(\nu) = \frac{\alpha}{T^2}\left\langle \frac{T}{(1 + 4\pi^2\lambda_0^2\nu^2)^2} + \frac{\tau_0}{(1 + 4\pi^2\lambda_0^2\nu^2)^3} \times \left\{\exp\left[-\frac{T}{\tau_0}(1 + 4\pi^2\lambda_0^2\nu^2)\right] - 1\right\}\right\rangle. \tag{53}$$

The dimensionless error variances are reduced inversely by the number of visits. This design for a ground-truth experiment is that of a low-altitude satellite that visits a site with a point gauge, taking a difference between satellite measurements and point gauge, then returning at intervals that ensure statistical independence until

the entire period (e.g., 1 month or 2 months) is covered. The average error variances are then

$$W_{NT}^2 = \frac{W_{1T}^2}{N}, \tag{54}$$

$$V_{NT}^2 = \frac{V_{1T}^2}{N}, \tag{55}$$

where N is number of visits during the entire period. When we consider a one-month period, we have $N \sim 60$ since the revisit interval of satellite is about 12 h. In practice $N < 60$ since the ground swath of the satellite often misses the gauge. The frequency of missing depends on swath width, orbit inclination, latitude, etc.

For a given shape of the footprint that is presented in section 2a, the DRMSE (dimensionless root-mean-square error) W_{1T} of 10-min column averages is shown in Table 1. We also give W_{60T}, which considers 60 visits over approximately one month in Table 1. We can see the effect of time averaging of different durations in Fig. 1. The rectangle FOV with 20 km × 20 km is used and the time averages range from 1 to 10 min. We see that the results are rather insensitive to the length of the averaging interval.

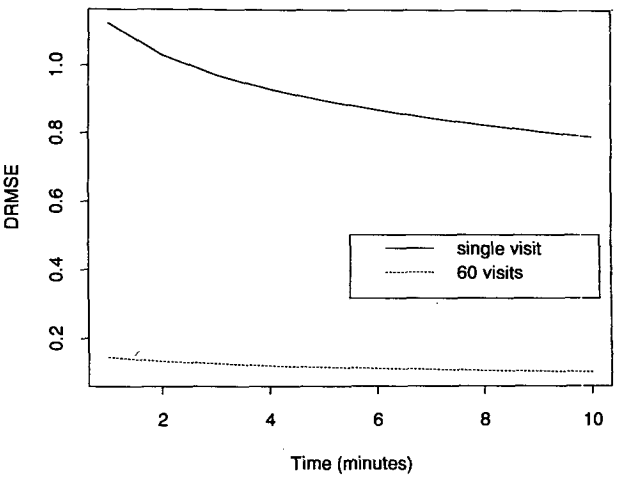

FIG. 1. The DRMSE (dimensionless root-mean-square error) for noise-forced diffusive precipitation model tuned to GATE for several-minutes averaging: comparing the point gauge with rectangular 20 km × 20 km FOV. The rms error is normalized to the standard deviation of FOV average fluctuations (climatology). Note that the normalization differs from Table 1.

4. Conclusions

In this paper we have seen that it is practical to compare point raingage measurements of rain rate with those made for an individual FOV of a microwave radiometer on board a satellite provided that the raingage measurements are smoothed over a few minutes. The temporal smoothing considerably reduces the small-scale variability in the rain field and imitates to some extent the vertical average of rain rate as seen by the satellite. A single pair of measurements is likely to contain a large component of random error due to the difference between a point and an area average measurement. Also the gauge will be located at random within the FOV on any given visit. However, when about 60 measurement pairs are aggregated the root-mean-square deviation reduces to about 10% (of the climatological standard deviation). This appears to be small enough to allow the technique to be used for identification of biases in the retrieval algorithms for individual FOVs.

The calculations are based upon a mean-square error formalism (North and Nakamoto 1989) that reduces the problem to an integral of the space–time spectral density weighted by design filters. As in other applications, this is extremely convenient since it separates issues concerning the experimental design from those that depend solely on the rain field characteristics (spectrum). Assumptions had to be made about both of these factors.

In the case of the rain field, we took it to be a stochastic field governed by a damped diffusion model forced by noise in space and time. While this model is fairly successful in reproducing the GATE rain statistics, it is still unrealistic, since among other things it does not exhibit the intermittency of real rain. We used the model parameters derived from tuning to the GATE data and these are certainly not the same at different locations on the earth. We believe this calls

TABLE 1. The DRMSE (dimensionless root-mean-square error) for the noise-forced diffusive precipitation model tuned to GATE for 10-min averaging: comparing the point gauge with the 10-min average. The rms error is normalized to the standard deviation of 10-min-averaged raingage fluctuations (climatology).

Footprint	a (km)	b (km)	Area (km^2)	DRMSE W_{1T}	DRMSE with 1 month (W_{60T})
Rectangle	10	10	100	0.460	0.059
	10	20	200	0.563	0.073
	10	30	300	0.633	0.082
	20	10	200	0.563	0.073
	20	20	400	0.630	0.081
	20	30	600	0.681	0.088
	30	10	300	0.633	0.082
	30	20	600	0.681	0.088
	30	30	900	0.721	0.093
Circular	10		314.2	0.596	0.077
	20		1256.6	0.751	0.097
	30		2827.4	0.826	0.107
Ellipse	10	10	314.2	0.596	0.077
	10	20	628.3	0.691	0.089
	10	30	942.5	0.750	0.097
	20	10	628.3	0.691	0.089
	20	20	1256.6	0.751	0.097
	20	30	1884.9	0.794	0.102
	30	10	942.5	0.750	0.097
	30	20	1884.9	0.794	0.102
	30	30	2827.4	0.826	0.107

for more research on rain fields, both theoretical and observational. Even so, we believe our results may be profitably used while we await more precise results in the future. The reason for our confidence is the fact that the results are rather insensitive to the actual averaging time employed. We would like to think of the 10% value as an upper limit. In fact, the result is likely to be less.

As to the design, we see ways to improve the ground configuration and are in the process of pursuing further calculations at this time. Some candidates include the following: 1) Two or more point gauges located a few km apart and within the FOV. 2) A row of gauges so that two or more gauges fall within each of a row of adjacent FOVs across the scan track. 3) A few-kilometer line average of rain rate as might come from a microwave attenuation device. The line average is less singular than a point gauge and might prove significantly superior to the point configurations. 4) There should be an appreciable advantage in stratifying the pairs based upon conditions. For example, we could omit all nonraining visits. We might also consider stratifying according to storm type to test the effect on different algorithms. These cases need to be examined in the context of different conditional spectra of rain-rate fields.

Acknowledgments. It is a pleasure to thank Kenneth Bowman and Thomas Wilheit for several helpful remarks that reminded us of the vertical averaging aspect of the satellite estimate and its equivalence to time averaging at the ground. Lianger Gong helped us with deriving formula (A6). We are also grateful for the support by grants from NASA, including the TRMM Science Team and basic research grants via the Atmospheric Dynamics and Radiation Branch.

APPENDIX

Derivation of $D_R(\nu)$ for Rectangular, Circular, and Elliptic Footprints

First, consider a rectangular footprint $R = [-a/2, a/2] \times [-b/2, b/2]$ in a Cartesian coordinate system. It may be easily found that

$$D_R(\nu) = G(\nu_x a)G(\nu_y b). \tag{A1}$$

For a circular footprint $R = \{(x, y) | r = (x^2 + y^2)^{1/2} < a\}$ of radius a in a polar coordinate system $D_R(\nu)$ is defined as

$$\begin{aligned} D_R(\nu) &= \frac{1}{A}\int_R \exp(2\pi i \nu \cdot \mathbf{r}) dR \\ &= \frac{1}{\pi a^2}\int_0^{2\pi}\int_0^a \exp(2\pi\nu r\cos\theta) r dr d\theta \\ &= \frac{1}{\pi a^2}\int_0^a\int_0^{2\pi} \cos(2\pi\nu r\cos\theta) r dr d\theta \\ &= \frac{2}{a^2}\int_0^a J_0(2\pi\nu r) r dr, \end{aligned} \tag{A2}$$

where $\nu = (\nu_x^2 + \nu_y^2)^{1/2}$ is the magnitude of ν, θ is the angle between $\mathbf{r}$ and ν, and $J_0(z)$ is the zero-order Bessel function. The above can be integrated further to obtain

$$D_R(\nu) = \frac{1}{\pi\nu a} J_1(2\pi a\nu), \tag{A3}$$

where $J_1(z)$ is the first-order Bessel function.

Finally for an elliptic footprint, $R = \{(x, y) | x^2/a^2 + y^2/b^2 < 1\}$ in a Cartesian coordinate system:

$$\begin{aligned} D_R(\nu) &= \frac{1}{A}\int_R \exp(2\pi\nu\mathbf{r}) = \frac{1}{\pi^2 ab\nu_x}\int_{-b}^{b} \\ &\quad \times \sin\{2\pi\nu_x a[1 - (y^2/b^2)]^{1/2}\} \exp(2\pi i\nu_y y) dy \\ &= \frac{2}{\pi^2 ab\nu_x}\int_0^b \sin\left[2\pi\nu_x \frac{a}{b}(b^2 - y^2)^{1/2}\right] \\ &\quad \times \cos(2\pi\nu_y y) dy. \end{aligned} \tag{A4}$$

This may be further reduced to

$$\begin{aligned} D_R(\nu) &= \frac{2}{\pi^2 a\nu_x}\int_0^{\pi/2} \sin(2\pi\nu_x a\cos\theta) \\ &\quad \times \cos(2\pi\nu_y b\sin\theta)\cos\theta d\theta. \end{aligned} \tag{A5}$$

The above integral expression can be written as

$$\begin{aligned} D_R(\nu) &= \frac{1}{\pi[(a\nu_x)^2 + (b\nu_y)^2]^{1/2}} \\ &\quad \times J_1\{2\pi[(a\nu_x)^2 + (b\nu_y)^2]^{1/2}\}. \end{aligned} \tag{A6}$$

The mathematical derivation of this formula is a very tedious task. We first expanded $\sin(2\pi\nu_x a\cos\theta)$ into a power series of $\cos\theta$ and the term $\cos(2\pi\nu_y b\sin\theta)$ into a power series of $\sin\theta$. Then we made use of the beta functions. Finally, the gamma functions and their factorial representations of integers were employed and (A6) was derived.

When $a = b$, the ellipse degenerates into a circle and (A6) degenerates into (A3).

REFERENCES

North, G. R., and S. Nakamoto, 1989: Formalism for comparing rain estimation designs. *J. Atmos. Oceanic Technol.*, **6**, 985–992.

Simpson, J., R. F. Adler, and G. R. North, 1988: A proposed Tropical Rainfall Measuring Mission (TRMM) satellite. *Bull. Amer. Meteor. Soc.*, **69**, 278–295.

Wilheit, T. T., and L. S. Chiu, 1991: Retrieval of monthly rainfall indices from microwave radiometric measurements using probability distribution functions. *J. Atmos. Oceanic Technol.*, **8**, 118–136.